

Modelling of Multiphase Flow in Pressure Swirl Atomizer

S.K. Amedorme

School of Mechanical Engineering, Institute of Thermofluids and Combustion, University of Leeds, UK

ABSTRACT

The internal flow in a pressure-swirl atomizer has been studied numerically. The atomizer is a generic design intended for internal combustion engines and is to be operated with liquid propane C_3H_8 as LPG is gradually replacing gasoline in internal combustion engines. The main objective of the work is to model the internal interaction of liquid propane (C_3H_8)-air flow in the atomizer using commercial code STAR-CCM+. Special emphasis is given to the flow of the liquid phase. Contour plots of axial and tangential velocities are obtained. The volume fraction of propane C_3H_8 and air are also presented. In addition, scalar scene of the vorticity is shown and analysed. Computational fluid dynamics, CFD, simulations have been performed in a three-dimensional, non-uniform grid on the atomizer and the computational domain. The liquid-air flow is modelled with the volume of fluid (VOF) multi-phase model in STAR-CCM+. The simulations manage to capture the overall flow characteristics in the pressure-swirl atomizer.

Key words: *Volume Of Fluid (VOF), Propane (C_3H_8), Vorticity, Axial and Tangential Velocities*

1. INTRODUCTION

Atomizers are used in many engineering applications including spray combustion in furnaces, diesel engines, direct injection petrol engines and gas turbine engines. They are also commonly used in applying agricultural chemicals to crops, paint spraying, spray drying of wet solids, food processing and cooling of nuclear cores. They are used to increase the specific surface area of the fuel and thereby achieve a high rate of mixing and evaporation. In most combustion systems reduction in mean drop size leads to higher volumetric heat release rate, easier ignition, a wide burning range and lower exhaust concentrations of the pollutant emissions. Atomizers are known to affect combustion stability limits, combustion efficiency, smoke and carbon monoxide generation, and unburned hydrocarbons [1, 2]. Pressure atomizers have different designs such as plain orifice, simplex, duplex, dual-orifice, fan spray and spill return. Pressure swirl atomizers also called simplex atomizers are the most versatile among them [3]. In all of them pressure swirl atomizers occupy a special position because they differ in quality of atomization, simplicity of construction, reliability of operation, low clogging and low expenditure of energy. However, the greatest disadvantages of these atomizers are that they require very high injection pressure and have low discharge coefficient owing to the fact the air core covers the majority of the atomizer orifice [4-6]. The basic principle of fluid flow through the swirl atomizer is that the liquid is introduced through tangential or helical passages into a swirl chamber from which it emerges through an exit orifice with a tangential velocity components. As a result of the vortex flow, a hollow air core is formed, it is concentric with the nozzle axis. The outflowing thin conical liquid sheet attenuates rapidly becoming unstable and disintegrates into ligaments and then drops in the form of a well-defined hollow cone spray [1]. Dombrowski and Hasson [6] also indicated that the motion in the swirl chamber is complex and the mechanisms of flow within the chamber and the resultant spray are not fully understood. Taylor [7] has shown that although the motion in the main stream can be considered irrotational, viscous effect on the retarded boundary layer cannot be neglected. The liquid in contact with the atomizer

walls cannot rotate fast enough to hold it in a circular path against the radial pressure gradient balancing the centrifugal motion and consequently a current directed towards the orifice is set up through the surface layer. Pressure swirl atomizer essentially consists of three main elements inlet tangential ports, swirl chamber and exit orifice. The exit orifice is preceded by a swirl chamber with a certain contraction or convergence. The inlet is one or more cylindrical or rectangular channels positioned tangentially to the swirl chamber as shown in Fig.1. The swirl chamber contains a strongly swirl motion of the liquid fuel and the central air core. In the chamber, a portion of the swirl energy is converted into axial velocity and the liquid fuel flows out of the nozzle in the form of a hollow cone. The exit orifice serves as the discharge outlet for the atomizer and contains holes in which the liquid is discharged. The size of the hole is usually of the order of a tenth of millimetre or less [8]. The internal flow of pressure-swirl atomizers has been studied numerically [9, 10]. The internal flow characteristics in pressure-swirl atomizers are important, because they govern the thickness of the sheet formed at the discharge orifice. It also governs the magnitude of the axial, tangential and radial velocity components of the sheet and hence the break-up of the film and characteristics of the resulting spray. The most important internal parameters in pressure swirl atomizers are: the pressure exerted by the fluid on the walls, the axial and the tangential components of the velocity and the air core characteristics. These characteristics significantly influence the discharge coefficient at the exit orifice, the spray cone angle and the liquid film thickness. The pressure on the internal walls of the atomizer also influences the swirling motion and the initiation of the central air core. Horvay and Leukel [10] observed that the pressure in swirl atomizer is almost constant in the swirl chamber, a sharp drop in the contraction zone and further decreases in the exist orifice. The liquid velocity is an essential factor that affects the degree of atomization and primarily depends on the injection pressure. The velocity has three components: the axial, tangential and the longitudinal. The formation of a central air core is another most important feature

of the flow in a simplex nozzle. The size of the air core determines the effective flow area at the discharge orifice and thus controls the coefficient of discharge, which is one of the important performance parameters of the nozzle [11].

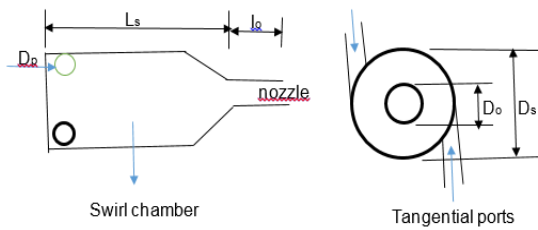


Fig.1. Pressure swirl atomizer schematic layout

Several approaches are used in the numerical analysis of multiphase flow in swirl atomizers. There are, among others, interface tracking methods, like: volume of fluid (VOF) [12, 13], level-set [14, 15] and front-tracking[16]. Volume of fluid (VOF) method used in this study has shown to be more flexible and efficient than other methods when treating complicated free boundary configurations. The VOF model is a simple multi-phase model that is well suited to simulate flows that consist of two or more immiscible fluids. The model assumes that all immiscible fluids present in each control volume share the same velocity, pressure and temperature fields. As a result of this assumption, the same set of basic governing equations describing momentum, mass and energy transport in a single-phase flow is solved for an equivalent fluid whose physical properties are calculated as function of its respective phases volume of fraction [17].

2. NUMERICAL SIMULATIONS

For a viscous three-dimensional flow, the flow is assumed to be governed by the Reynolds-averaged Navier-Stokes equations (RANS), in which the turbulence effects are included via eddy-viscosity model. In this case, the continuity equation, three momentum components equations, and two equations for turbulence properties are solved. The equations are:

Mass conservation

$$\frac{d}{dt} \int_V \rho dV + \int_S \rho v(v - v_b) \cdot n ds = 0 \quad (1)$$

Momentum conservation

$$\frac{d}{dt} \int_V \rho v dV + \int_S \rho v(v - v_b) \cdot n ds = \int_S (T - pI) \cdot n ds + \int_V \rho b dV \quad (2)$$

Generic transport equations for scalar quantities

$$\frac{d}{dt} \int_V \rho \phi dV + \int_S \rho \phi(v - v_b) \cdot n ds = \int_S \Gamma \nabla \phi \cdot n ds + \int_V \rho b_\phi dV \quad (3)$$

where ρ stands for fluid density, v is the fluid velocity vector and v_b is the velocity of the CV surface, n is the unit vector normal to the CV surface with area S and volume V . T stands for the stress tensor (expressed in terms of velocity gradient and eddy viscosity), p is the pressure, I is the unit tensor, ϕ stands for the scalar variable, $\Gamma = 0.7$ is the diffusivity coefficient, b is the

vector of body forces per unit mass and b_ϕ represents sources and sinks of ϕ [18].

To account for the free surface and allow for arbitrary deformation, an additional equation needs to be solved for the volume fraction α of the liquid phase (C3H8)

$$\frac{d}{dt} \int_V \alpha dV + \int_S \alpha(v - v_b) \cdot n ds = 0 \quad (4)$$

The liquid propane (C3H8) and (air) are considered as two immiscible components of a single effective fluid, whose properties are assumed to vary according to the volume fraction of each component as follows for the density ρ and viscosity μ :

$$\rho = \rho_1 c + \rho_2(1 - \alpha) \quad (5)$$

$$\mu = \mu_1 c + \mu_2(1 - \alpha) \quad (6)$$

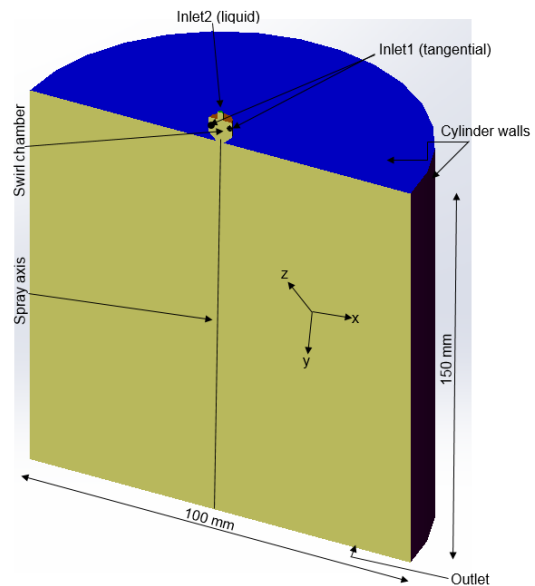


Fig.2. Geometry and boundary conditions, three-dimensional

Computations are performed courtesy of the CFD code STAR CCM+10.02.010-R8 for Windows 64 .The equations (1)-(6) are solved using the finite-volume method in association with the SIMPLE algorithm and the Second Order Upwind scheme. The SIMPLE algorithm uses a relationship between velocity and pressure corrections to enforce mass conservation and to obtain pressure field. The Second Order discretization is more accurate than the First Order upwind scheme and more suited for practical engineering problems. Two equations standard k-ε model has been adopted for the computation of turbulence in the fluids since there is no conclusive information available in the literature concerning accurate and suitable modification of the k-ε model for multiphase flow. The geometry shown in Fig.2 was created using CAD package (Solidworks) and imported into the STAR-CCM+. The model consists of two parts the nozzle part which is attached to the computation domain just to study the flow at the exist orifice of 2mm in diameter. The computation domain dimensions are large so that the outlet boundary conditions do not affect the flow.

Three-dimensional calculations are carried out on the flow through the velocity inlet2 of 2mm diameter with density of propane liquid ($\rho_l = 800kg/m^3$) and density of air ($\rho_a =$

$1.30\text{kg}/\text{m}^3$) through velocity inlet1 having 2mm of diameter as shown in Fig.3. The walls represent the solid walls of the nozzle and the computation domain. The standard wall functions are used to model the near-wall regions with no-slip conditions. Pressure outlet is specified for the flow out. The inlet boundary conditions used to perform the calculations for the liquid are: 3bars for the injection pressure, 1 for volume fraction, 10% for turbulent intensity, 0.04 mm for turbulent length scale and 10.0 m/s for the velocity magnitude. And for the air inlet the value remains the same except for the velocity magnitude which is 100 m/s. The outlet boundary conditions are 1% for turbulent intensity, volume fraction of one for both liquid and air and 0.01m for the turbulent length scale. A non-uniform mesh grid composed of 54720 tetrahedral cells is used for the computation and shown in Fig.4. The distribution of the mesh was done such that the swirl chamber and the cylinder have fine and coarse meshes respectively. The refined grid spacing on the swirl chamber was about 0.15 mm and a coarse mesh of 1.0 mm on the computation domain with a growth factor of 2.0. This is to reduce the computational time and for the 3.20GHz Intel(R) Xeon(R) processor to accommodate. The total computational time was about two (2) days.

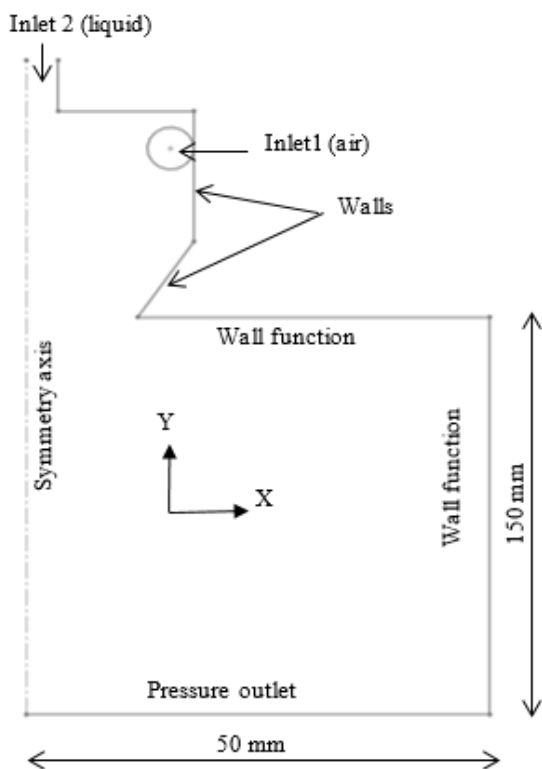


Fig.3. Geometry and boundary conditions, two-dimension



Fig.4. Computational grid, three-dimensional.

3. RESULTS AND DISCUSSION

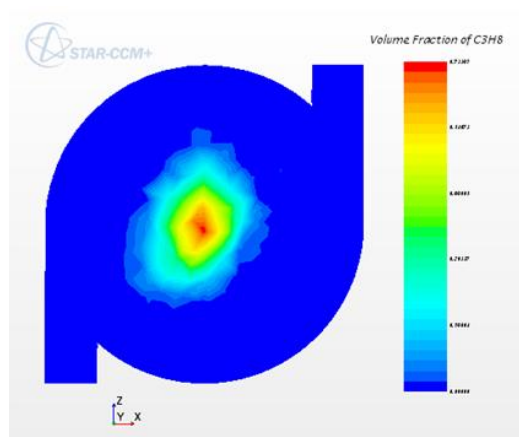


Fig.5. Contour plot of volume fraction of propane on the cross-sectional plane

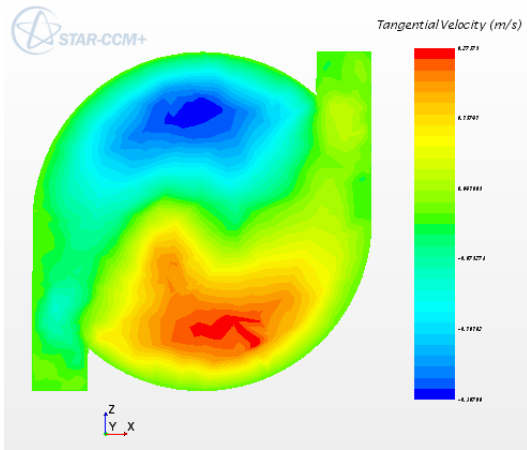


Fig.6. Contour plot of tangential velocity on cross-sectional plane

The Fig.5 shows the contour plot of volume fraction of propane on cross-sectional plane. The volume fractions are colour coded such that the red represents the maximum and the blue indicates the minimum volume for the liquid. The volume of fraction is 1 and 0 for the liquid and air phase respectively. It can be observed that the liquid volume fraction is quite symmetrical on the spray axis. Fig.6 shows the tangential velocity distribution on the cross plane through the swirl chamber. Maximum and minimum tangential velocities can be observed diametrically opposite.

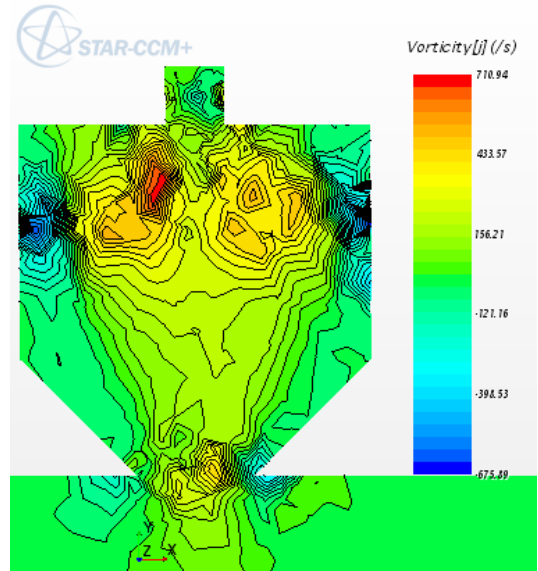


Fig.8. Vortices in the atomizer visualised by path lines

On the vertical plane through the pressure swirl atomizer Fig. 7 shows the contour plot of the axial velocity obtained in the numerical simulation. Regions of higher velocity in the liquid are found near the wall. The liquid passes the concave wall, giving rise to hydrodynamic instabilities which result in the formation of the vortices as visualized by the path lines shown in Fig. 8.

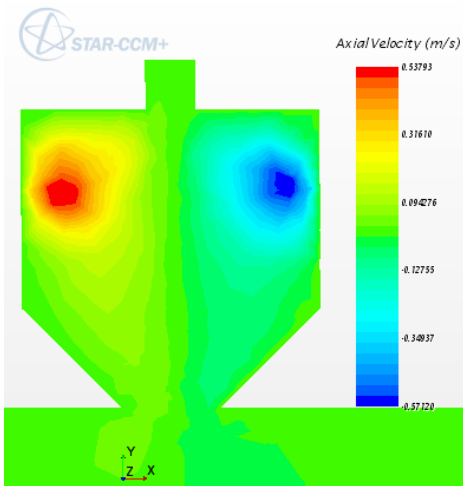


Fig.7. Axial velocity scene within the atomizer

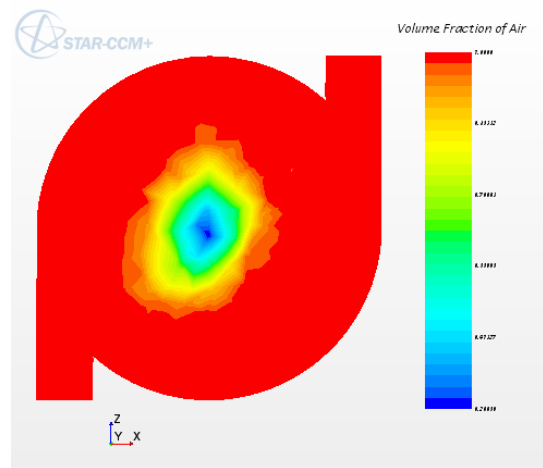


Fig. 9. Contour plot of volume of fraction of air on the cross-sectional plane

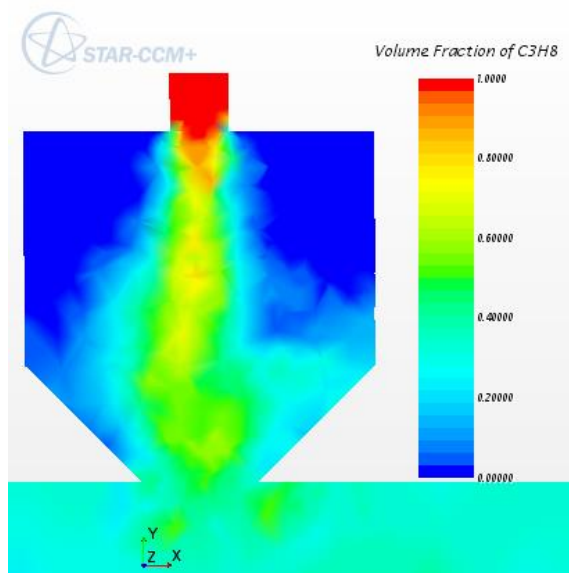


Fig.10. Volume fraction of propane on the vertical plane

Fig.10 presents the volume fraction of propane (C₃H₈) on the vertical plane. The liquid core in the middle (yellow and green) is induced by the motion of the air shown in Fig.9. The volume is maximum in the vicinity of the inlet, indicated in the red colour, and decreases towards the exit orifice. Qualitatively, the diameter of the liquid is slightly larger in the convergent part of the chamber than its size in the swirl chamber and reduces in size at the exit orifice. This is in general agreement with De Keukelare [8] who experimentally discovered that there is a slight reduction in diameter of fluid within the outlet of the convergence and exit orifice, and is attributed to the a vena contracta effect, due to the liquid having to negotiate a sharp bend. The interface between the propane (C₃H₈) and air becomes unsteady displaying waves of small amplitude along its surface. The waves originate at the stagnation point and propagate towards the exit. Their amplitude seems to be increasing with decreasing axial distance. After exit, violent movement is noticed between the liquid propane (C₃H₈) and the air.

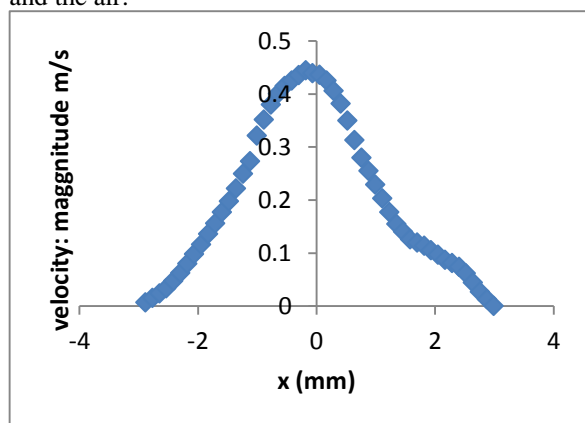


Fig.11. Profile of velocity magnitude on a horizontal line across the swirl chamber

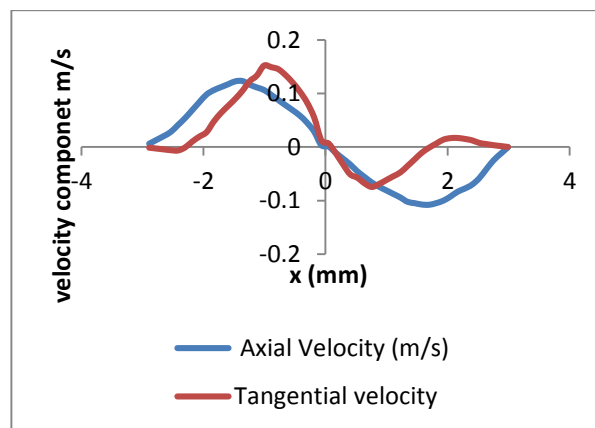


Fig.12. Axial and tangential velocity profile in the swirl chamber

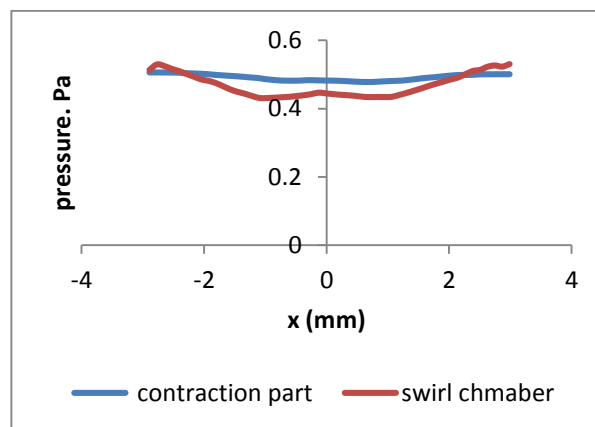


Fig.13. Pressure profile of the liquid on the internal walls of the atomizer

Fig.11. shows the graphs of velocity magnitude for the various positions on a horizontal line drawn across the section plane. It can be observed that the velocity magnitudes are high at the centre positions and decrease quite linearly towards the swirl chamber walls. The general profile of the velocity magnitudes, taken on the probe line across the section plane, is quite similar to the measured velocity profiles at the inlet level by Horvay and Leuckel [10]. The radial distance distribution of the axial and tangential velocities of the liquid in the pressure swirl atomizer is shown in Fig.12. It is observed that the tangential component of the velocity is relatively higher than axial velocity in the swirl chamber although it falls below the axial velocity slightly towards the walls in the swirl chamber. The pressure distributions of the liquid on the internal walls of the atomizer, for the swirl chamber and contraction regions, are compared and presented in Fig.13. It is deduced from the graph that the pressure is higher in the contraction region than the swirl chamber.

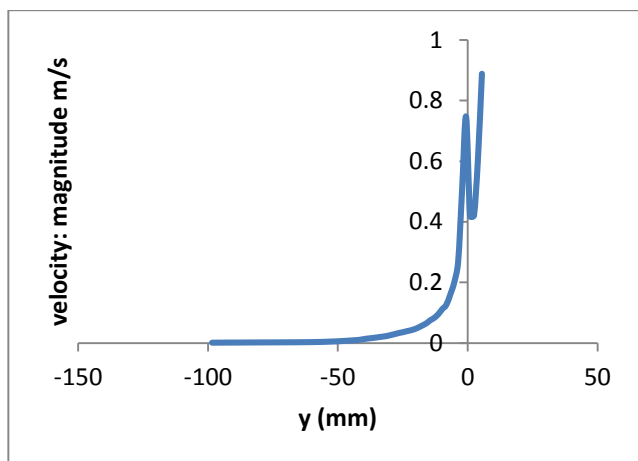


Fig.14. Velocity magnitude on symmetry line on the vertical plane

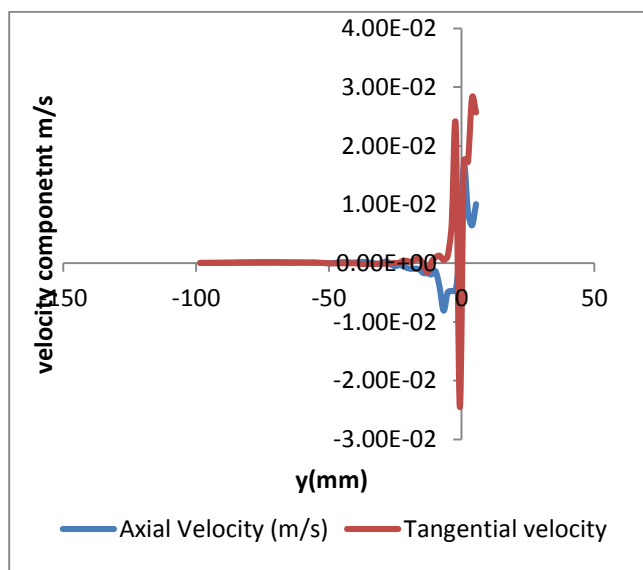


Fig.15. Velocity components on symmetry line on the vertical plane

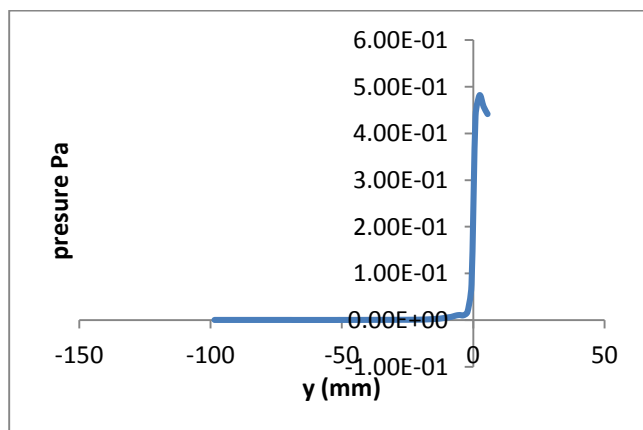


Fig.16. Pressure profile on symmetry line on the vertical plane

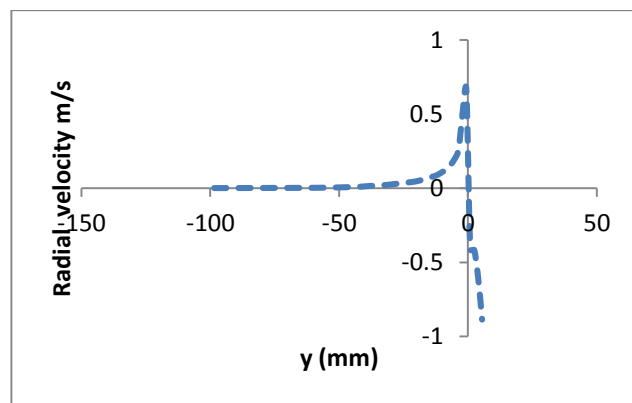


Fig. 17. Radial velocity on symmetry line on the vertical plane

Fig.14 presents the graph obtained for the velocity magnitudes on the spray axis (symmetry axis). The velocity magnitudes are higher in the atomizer and decrease in the computational domain. The other parameters such as axial and tangential velocities, pressure and radial velocity show similar trends on the symmetry axis on the vertical plane (Figs.15 -17).

4. CONCLUSION

Multiphase modelling in pressure swirl atomizer is done with CFD commercial code STAR-CCM+ using the volume of fluid (VOF) approach in modelling the internal characterises of pressure swirl atomizer. Scale scene of volume fraction of the liquid propane and air as well as vorticity have been shown. Axial and tangential velocities resulting from the flow have been presented and analysed. The general profiles of the results are similar to the trends in the literature.

REFERENCE

Lefebvre, A., Atomization and sprays. Vol. 1040. 1989: CRC press.

Lefebvre, A.H. and D. Hallal, Gas Turbine Alternative Fuels and Emissions. CRC, Boca Raton, FL, 2010.

Lefebvre, A.H., Gas turbine combustion. 1998: CRC press.

Khavkin, Y.I., Theory and practice of swirl atomizers. 2003: CRC Press.

Bayvel, L. and Z. Orzechowski, Liquid Atomization, Combustion: An International Series. 1993, Taylor & Francis.

Dombrowski, N. and D. Hasson, The flow characteristics of swirl (centrifugal) spray pressure nozzles with low viscosity liquids. AIChE Journal, 1969. 15(4): p. 604-611.

Taylor, G., The boundary layer in the converging nozzle of a swirl atomizer. The Quarterly Journal of Mechanics and Applied Mathematics, 1950. 3(2): p. 129-139.

De Keukelaere, H., The Internal Flow in a Swirl Atomizer Nozzle. 1995.

Yule, A. and J. Chinn, The internal flow and exit conditions of pressure swirl atomizers. *Atomization and Sprays*, 2000. **10**(2): p. 121-146.

Horvay, M. and W. Leuckel, Experimental and theoretical investigation of swirl nozzles for pressure-jet atomization. *German chemical engineering*, 1986. **9**(5): p. 276-283.

Datta, A. and S. Som, Numerical prediction of air core diameter, coefficient of discharge and spray cone angle of a swirl spray pressure nozzle. *International journal of heat and fluid flow*, 2000. **21**(4): p. 412-419.

Hirt, C.W. and B.D. Nichols, Volume of fluid (VOF) method for the dynamics of free boundaries. *Journal of computational physics*, 1981. **39**(1): p. 201-225.

Ménard, T., S. Tanguy, and A. Berlemont, Coupling level set/VOF/ghost fluid methods: Validation and application to 3D simulation of the primary break-up of a liquid jet. *International Journal of Multiphase Flow*, 2007. **33**(5): p. 510-524.

Sethian, J.A., *Level set methods and fast marching methods: evolving interfaces in computational geometry, fluid mechanics, computer vision, and materials science*. Vol. 3. 1999: Cambridge university press.

Osher, S., R. Fedkiw, and K. Piechor, *Level set methods and dynamic implicit surfaces*. *Applied Mechanics Reviews*, 2004. **57**: p. 15.

Tryggvason, G., et al., A front-tracking method for the computations of multiphase flow. *Journal of Computational Physics*, 2001. **169**(2): p. 708-759.

Johannessen, S.R., *Use of CFD to Study Hydrodynamic Loads on Free-Fall Lifeboats in the Impact Phase.: A verification and validation study*. 2012.

Guide, U., *Star-CCM+ Version 8.04*. CD-adapco-2013, 2013.